



This is a repository copy of *Influence of backfill on the capacity of masonry arch bridges*.

White Rose Research Online URL for this paper:
<http://eprints.whiterose.ac.uk/78781/>

Version: Published Version

Article:

Callaway, P., Gilbert, M. and Smith, C.C. (2012) Influence of backfill on the capacity of masonry arch bridges. *Proceedings of the Institution of Civil Engineers: Bridge Engineering*, 165 (3). 147 - 157. ISSN 1478-4637

<https://doi.org/10.1680/bren.11.00038>

Reuse

Unless indicated otherwise, fulltext items are protected by copyright with all rights reserved. The copyright exception in section 29 of the Copyright, Designs and Patents Act 1988 allows the making of a single copy solely for the purpose of non-commercial research or private study within the limits of fair dealing. The publisher or other rights-holder may allow further reproduction and re-use of this version - refer to the White Rose Research Online record for this item. Where records identify the publisher as the copyright holder, users can verify any specific terms of use on the publisher's website.

Takedown

If you consider content in White Rose Research Online to be in breach of UK law, please notify us by emailing eprints@whiterose.ac.uk including the URL of the record and the reason for the withdrawal request.



eprints@whiterose.ac.uk
<https://eprints.whiterose.ac.uk/>

Influence of backfill on the capacity of masonry arch bridges

■ **Phillip Callaway** MEng, PhD, CEng, MICE
Vice-Professor, School of Civil Engineering, Henan Polytechnic University, China

■ **Matthew Gilbert** PhD, CEng, MICE, MASCE
Reader, Department of Civil and Structural Engineering, University of Sheffield, UK

■ **Colin C. Smith** MA, PhD
Senior Lecturer, Department of Civil and Structural Engineering, University of Sheffield, UK



The influence of the presence of backfill on the load-carrying capacity of a masonry arch bridge can be considerable. The backfill is responsible for transmitting and distributing live loads from the road or rail surface through to the arch barrel and also for laterally stabilising the arch barrel as it sways under load. However, it can be difficult to separate these two distinct effects, and hence also difficult to ascertain whether existing assessment code recommendations are realistic. To address this, a series of experiments designed to separate these two effects have been performed. A total of 27 small-scale bridge tests were undertaken and the experimentally obtained peak loads then compared with results from limit analysis software of varying complexity. It was confirmed that passive restraint and live load distribution both contribute significantly to bridge-carrying capacity, and that, when failure involves a four-hinge failure mechanism, even comparatively simple limit analysis software can model the various effects remarkably well.

1. Introduction

Masonry arch bridges continue to form a vital part of the transport infrastructures of the UK and many other countries around the world. However, many aspects of their behaviour remain poorly understood. For example, it has been known for at least a century (Alexander and Thomson, 1900) that the soil backfill material placed around the barrel of a masonry arch bridge in order to provide a level road or rail surface can have a significant beneficial effect on its ultimate load-carrying capacity, over and above the 'pre-stressing' effect arising from the self-weight of the soil. However, quantifying this reliably has proved challenging.

To date, assessment codes and purpose written masonry arch analysis software programs have generally attempted to quantify the beneficial effects of backfill by using simplified models which account separately for: (a) distribution/spreading of the live load through the backfill, and (b) passive restraint which helps prevent sway of the arch barrel into the surrounding backfill material (Figure 1). Although this approach makes it unnecessary to separately model both masonry and soil backfill

components of a bridge directly, in a potentially complex coupled soil–structure interaction model, it does require the analyst to choose judiciously values for the various semi-empirical modelling parameters involved (or to verify that the default values used in third party software are reasonable).

While the use of such semi-empirical parameters in engineering practice is commonplace, a particular problem here is that in a load test to collapse on a masonry arch bridge both live load distribution and passive restraint effects will be involved, making it very difficult to ascertain their relative importance. For example, a good prediction of the ultimate load-carrying capacity of a bridge can be obtained even if the degree of live load distribution is significantly over-estimated, provided the degree of passive restraint is under-estimated (or vice-versa). Since the relative importance of the two effects is likely to change from bridge to bridge, this situation is clearly unsatisfactory. This paper therefore describes details of what are believed to be the first series of experiments designed with the specific aim of decoupling the beneficial effects of live load distribution and passive restraint in soil-filled masonry arch

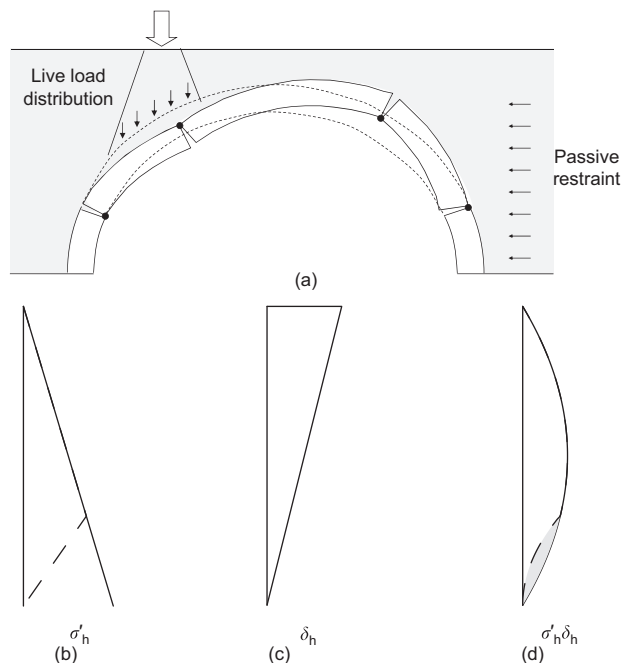


Figure 1. (a) Two beneficial effects of soil backfill in a masonry arch bridge: live load distribution/spreading and passive restraint, (b) assumed horizontal passive pressure distribution with depth down to lower hinge point (dashed line indicates Burroughs *et al.* (2002) proposed bilinear cut-off), (c) assumed horizontal displacements on passive side, (d) energy dissipation per unit area (dashed line indicates deviation when using Burroughs *et al.* bilinear cut-off)

bridges. Results from the tests are then compared with predictions from limit analysis software of varying complexity.

2. Background

Limitations in the predictive capability of traditional arch bridge assessment techniques (e.g. the long-established MEXE method of assessment (Highways Agency, 2001a), which does not account for the competence of the backfill material used, and which also relies on numerous other simplifications (Wang and Melbourne, 2010)) are stimulating the development of arguably more rational analysis and assessment techniques for arch bridges. As soil backfill has been found experimentally to contribute significantly to bridge load-carrying capacity (e.g. see Figure 2, which indicates that the load-carrying capacity of a soil-filled bridge can be in excess of 10 times that of a comparable bare arch barrel (Melbourne and Gilbert, 1995)), it follows that due attention needs to be paid to the issue of soil-arch interaction when formulating any replacement for traditional arch bridge assessment techniques.

Considering distribution of live load through the backfill (see Figure 1(a)), the field load tests conducted many years ago by

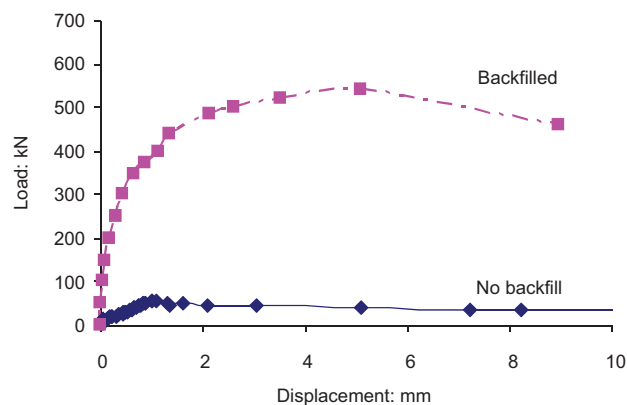


Figure 2. Influence of presence of soil backfill on load-carrying capacity as identified experimentally (3 m span, 0.215 m thick segmental arch barrel with 4:1 span:rise ratio and 0.3 m granular backfill above crown) (after Smith *et al.*, 2004)

Davey (1953) and Chettoe and Henderson (1957) appear to indicate that certain types of masonry arch bridge backfills might distribute the live load better than others. Application of geotechnical engineering principles also indicate that this should be the case (e.g. see BS 8004 (BSI, 1986)). However, current UK codes of practice recommend that the live load is distributed longitudinally according to a simple 'one size fits all' approach, assuming a 'one horizontal to two vertical' distribution model (Highways Agency, 2001b; Network Rail, 2006). Very little research appears to have been undertaken to justify this, and workers such as Harvey (2006) have suggested the whole area demands urgent re-evaluation.

Considering next passive restraint (see Figure 1(a)), while such restraint is generally assumed to be present there are uncertainties as to how the magnitude and distribution of restraining pressures should be established. The most common assumption is to adopt a Rankine style triangular pressure distribution (Figure 1(b)), with the coefficient of passive resistance computed for a vertical frictionless wall, K_p , being factored down to account for the fact that the arch barrel is curved rather than vertical, is rough rather than smooth and also that, at the point at which the peak load is reached, movements of sections of the arch barrel into the backfill will be much lower than those needed to mobilise full passive pressures. Also, since movement of the arch barrel into the backfill becomes vanishingly small close to the hinge furthest from the applied load (assuming a four-hinge mechanism), significant passive pressures cannot be expected to be mobilised here. Thus Burroughs *et al.* (2002) added a cut-off to the standard Rankine style distribution to correct for this, thereby transforming the standard triangular passive pressure distribution into a bilinear one (Figure 1(b)). However, when

computing the load-carrying capacity the effect of such a cut-off on predicted load-carrying capacity will generally be relatively small. This is because the structural displacements close to the hinge (Figure 1(c)) are small, and so the work done here (Figure 1(d)) will also be relatively small even if large Rankine style pressures are present. It is therefore debatable as to whether the benefits of introducing such a cut-off warrant the additional complexity introduced (for example, an assumed cut-off at 0.3 of the full height of a rotating arch segment results in a modest 9% reduction in work done).

In order to develop a fuller understanding of these issues, a series of tests on full and small (1/8th) scale soil-filled model arch bridges have recently been undertaken at the Universities of Salford and Sheffield. Small-scale bridges are inexpensive and quick to build and test (as noted by, for example, Fairfield and Ponniah, 1994). Thus small-scale models can be used to rapidly investigate a wide range of parameters, with results then corroborated as necessary using the full scale apparatus (Gilbert *et al.*, 2007).

Results from a study undertaken using the small scale test apparatus specifically designed to separate live load distribution and passive restraint effects are described in this paper; details of the full-scale tests are provided elsewhere (Gilbert *et al.*, 2010). Various numerical models are used to help interpret the results obtained, with tentative recommendations for practice then made.

3. Laboratory test programme

All tests were carried out using a purpose made clear-sided cast acrylic test chamber reinforced with steel, as previously

successfully used to investigate the influence of flooding on load-carrying capacity (Hulet *et al.*, 2006). Each model arch bridge had a span of 380 mm and comprised 25 voussoirs, as shown in Figure 3, which shows the standard test set-up used. The selected backfill was dry sand which could readily be poured using pluviation. The load was applied through loading screws via a load bracket onto the backfill. This meant that the applied load was controlled by the vertical displacement of the load plate.

Prior to backfilling, silicon grease was used at the interface between the edges of the arch and the side walls of the rig to prevent sand particles becoming lodged there. The weighed backfill was placed by pluviation from a height of 422 mm to achieve the depth of backfill required, to the density given in Table 1. Upon removal of the centring, loading was then applied at the quarter point using a load plate connected to a simple hand screw arrangement, with the intensity of the load recorded by two electrical resistance-strain-gauge type load cells. Each full turn of a load screw corresponded with a vertical downward displacement of 1.6 mm. After each displacement increment a photograph was taken with a digital camera to create a series of images which were then analysed using particle image velocimetry (PIV) to obtain soil displacement vectors enabling the soil failure mechanism to be visualised (White *et al.*, 2001).

In order to maintain maximum transparency of the side walls for the visual imaging technique used, no attempt was made to reduce the boundary friction interface between the sand and the clear cast acrylic side walls, though additional experimental work was undertaken to quantify the friction angle at this surface, determined to be approx. 8° (see Callaway (2007) for details).

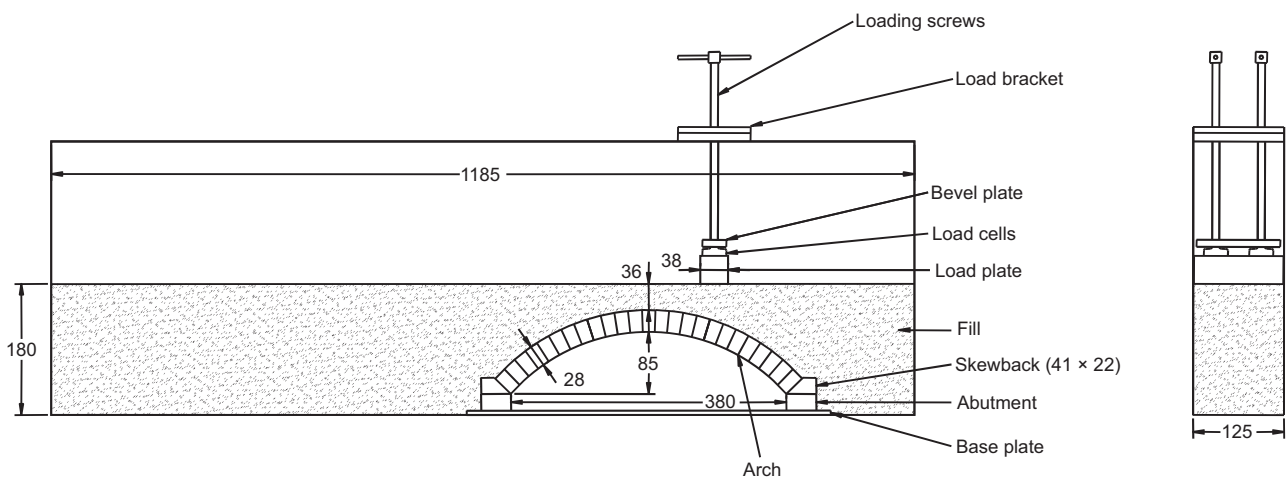


Figure 3. Apparatus set-up and dimensions (all dimensions in mm). Note: the geometrical properties indicated are more accurate than those given in Callaway (2007), where small inaccuracies in the values used in subsequent modelling studies coloured the conclusions drawn.

Material	Property	Value	Units	Notes
Sand	Soil friction angle, ϕ'	43.8	degrees	Derived from 100 × 100 mm direct shearbox tests
	Cohesion, c'	0	kPa	
	Void ratio	0.58		Estimated value
	Bulk unit weight, γ_{rig}	16.5	kN/m ³	Derived from in-situ sampling via soil sampling tins – Figure 4(a)
Sand–acrylic interface	Moisture content	<1	%	Sand was oven dried before tests
	Interface friction angle, δ	8	degrees	Derived from in-rig test (side walls only; voussoir-sand surfaces roughened)
Acrylic	Unit weight	13.7	kN/m ³	Manufacturer's value

Table 1. Material properties

Additional tests using deflection gauges on the side walls of the tanks showed deflections of < 0.1 mm over the test chamber width of 125 mm, indicating that near-plane strain conditions were achieved within the test rig during each experiment.

The main objective of the laboratory test programme was to devise and conduct tests which would allow the various effects of the backfill on bridge load-carrying capacity to be isolated. This was achieved by devising ways of removing each of the various effects.

- First, live load distribution effects were in some tests removed by applying the load directly onto the arch barrel.
- Second, passive restraining pressures were in some tests removed by omitting fill beyond the springing furthest from the load, and placing backfill on the unloaded side of the bridge within semi-rigid bags. Two bags were used to contain the requisite volumes of fill, resting on the barrel either side of the expected location of the relevant span hinge (between voussoirs 9 and 10). This provided an appropriate ‘balancing weight’, against which the applied load could react.
- Third, active pressures were in some tests removed by omitting backfill from the loaded side of bridge and using an extended keystone to contain backfill placed on the unloaded side. (In this case no attempt was made to replicate the dead weight of the fill.)

This led to a total of six main test set-ups (T1–T6), each of which incorporated an extended keystone voussoir. However, in order to verify the (anticipated minimal) influence of the extended keystone voussoir, repeat test set-ups which did not incorporate the extended keystone voussoir were used where this element was not essential to restrain backfill. The main test set-ups are shown in Table 2 and further details of test set-up T2 incorporating an extended keystone voussoir is shown in Figure 4. For each set-up a total of three (or six) tests were performed in order to assess repeatability, giving 27 tests in total.

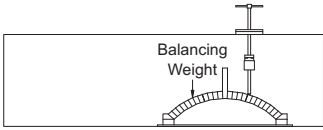
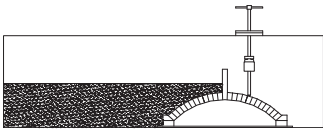
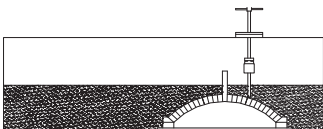
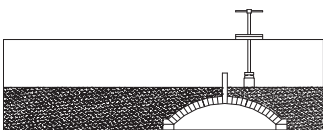
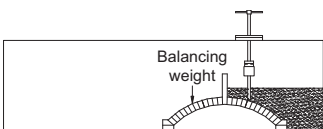
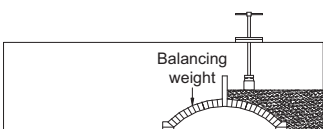
In the case of test set-ups with load distribution effects removed – set-ups T1 [---], T2 [-P-], T3 [AP-] and T5 [A--], the load was applied directly to a voussoir by applying a pair of 2 mm diameter rods to the extrados of the arch, as shown in Figure 4. This was assumed to be equivalent to the load being applied over an area of a 2 mm wide strip running the full width of the arch extrados since each voussoir extended across the full width of the bridge.

3.1 Material properties

The properties of the test materials were experimentally determined using procedures described in Head (1982), and are shown in Table 1 and Figure 5. The dry sand used as backfill had a particle size range of approx. 0.5 mm–1.0 mm. Though this material is not physically representative of backfill typically encountered in the field, the angle of friction (43.8°) is broadly representative, and the use of sand does enable consistent beds of material to be readily prepared for each test, an important consideration in physical modelling. In addition the ratio of loading plate width to average particle size is greater than 35, ensuring particle size effects are minimal.

4. Test results

The experimental results obtained for the six main test set-ups are summarised in Table 3. By comparing results from tests T1 [---] and T2 [-P-] and also T3 [AP-] and T5 [A--], the beneficial influence of passive restraint is clear (31% and 35% increases respectively). Similarly by comparing results from tests T3 [APL] and T4 [APL] and also T5 [A--] and T6 [A-L] the beneficial influence of applying the live load on top of the backfill, rather than directly to the arch barrel, is clear (32% and 29% increases respectively), although it should be noted that this increase is in part due to the increased loaded length (38 mm *cf.* 2 mm), rather than being solely due to load spreading. Other observations included: (a) by ensuring the testing procedure was carefully controlled, highly repeatable results could be obtained, and (b) the extended keystone voussoir had negligible influence on the results (results for variants on test set-ups T1, T3, T4 in

Test [Key*]	Arrangement	No. of tests [No. without extended keystone]	Description
T1 [---]		3 [3]	<ul style="list-style-type: none"> ■ No active fill ■ Passive fill represented by dead load only ■ No live load distribution
T2 [-P-]		3	<ul style="list-style-type: none"> ■ No active fill ■ Full passive fill ■ No live load distribution
T3 [AP-]		3 [3]	<ul style="list-style-type: none"> ■ Active fill ■ Passive fill ■ No live load distribution
T4 [APL]		3 [3]	<ul style="list-style-type: none"> ■ Active fill ■ Passive fill ■ Full live load distribution
T5 [A--]		3	<ul style="list-style-type: none"> ■ Active fill ■ Passive fill represented by dead load only ■ No live load distribution
T6 [A-L]		3	<ul style="list-style-type: none"> ■ Active fill ■ Passive fill represented by dead load only ■ Full live load distribution

*A = active; P = passive; L = load spreading

Table 2. Masonry arch bridge test set-ups

which the extended keystone voussoir was not utilised are shown in square brackets in Table 3).

The use of the adopted visual imaging technique was found to work well. Photographs from the series of tests were each analysed using PIV. Table 3 shows PIV images produced for each test, showing superimposed displacement vectors at peak load.

The use of PIV can also be used to further investigate the influence of the extended keystone. Thus Figure 6 shows superimposed displacement vectors obtained for test set-up T4. As can be seen, including an extended keystone appears to have a relatively small effect on the observed soil–arch interaction behaviour. However, when the extended keystone is present the centre of rotation does appear to be slightly nearer to the crown, and any tendency for soil over the crown of the arch to be involved in a partial bearing capacity failure is

suppressed, with this forced (reflected) to the non-preferred side. However, as noted previously, this was found to have a very small effect on the peak load-carrying capacity of the model bridges (approx. 2%).

Figure 7 shows averaged load–displacement curves for the arch bridge tests, showing vertical displacement of the loading plate and of the voussoir directly below this. Error bars are included which indicate the full range of results obtained from the three repeat tests. All displacements were obtained using PIV, by extracting the vertical component of the displacement vectors of the load plate and the appropriate voussoir.

Although for a given test set-up it is evident from Table 3 that there was a high degree of consistency in the experimentally recorded peak load, from Figure 7 it is evident that there was some variability in the observed load-displacement responses,

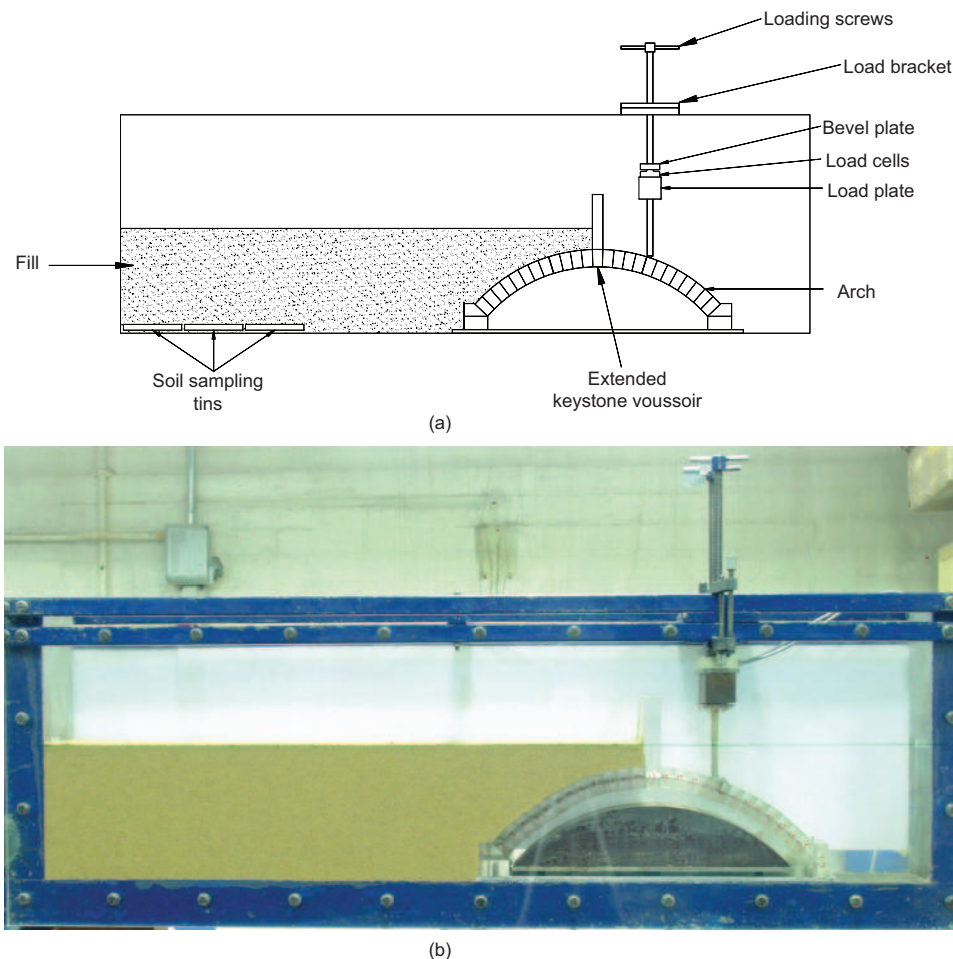


Figure 4. Test apparatus incorporating extended keystone voussoir (set-up T2 – passive restraint only): (a) general arrangement, (b) photograph

largely owing either to non-repeatable bedding-in of the load plate (relevant to test set-ups T4 and T6), or due to the load screws sliding on the extrados of the arch barrel near the end of a given test, when gross deformations of the arch barrel were involved (relevant to test set-ups T1, T2, T3 and T5).

5. Numerical simulations

5.1 Rigid block limit analysis

The experimentally observed peak loads were compared with predictions obtained using the LimitState:RING 3.0 analysis software (LimitState, 2011). In this software masonry blocks are modelled explicitly, using the rigid block analysis technique (Gilbert and Melbourne, 1994; Livesley, 1978) and exact limit analysis solutions for a given discretisation of voussoirs can be obtained. However, a simplified, indirect, soil model is employed in the software which requires semi-empirical load

dispersion and passive restraint properties to be specified. Measured geometrical and unit weight properties were used in all analyses.

In this study the default truncated Boussinesq load distribution model was used initially (see LimitState (2011) – relevant only to test set-ups T4 [APL], T6 [A–L]). In the software it is assumed that active pressures are small, so are ignored. The degree of passive restraint was determined by the software from the measured angle of friction of 43.8° (relevant in the case of test set-ups T2 [-P-], T3 [AP-], T4 [APL] only). The software uses a Rankine style triangular pressure distribution with a default passive pressure mobilisation factor of 0.33 (i.e. corresponding to 1/3 of the classical passive earth pressure coefficient on a smooth vertical wall for a material with an angle of friction of 43.8°). Results are included in Table 3 and it is evident that, considering the comparative simplicity of the

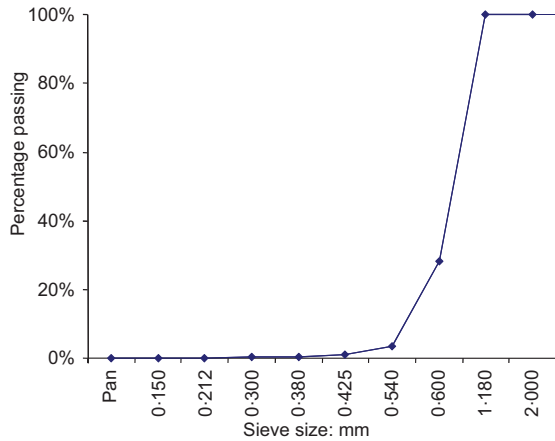


Figure 5. Particle size distribution for the sand backfill

model, the predictions are remarkably good (all within 10% of the experimental results).

It was considered of interest to also analyse test set-ups T4 and T6 using a 2:1 (vertical:horizontal), uniform load distribution of the sort advocated in BA16/97 (Highways Agency, 2001a). It was found that the use of such a distribution led to over-estimates of bridge strength of 14% and 11% (cf. 4% and 3% when using the default truncated Boussinesq model), suggesting that this distribution model is non-conservative. (Note also that for this study the horizontal extent of the load on the arch barrel was calculated from the width of the load w and the depth of fill h below this, i.e. loaded length = $w + h$. However, BA16/97 indicates that load should be dispersed onto the arch centreline, acting on all segments of the arch which fall within 2:1 dispersal lines. For a curved arch of finite thickness this will lead to even greater distribution, and to even more non-conservative predictions of bridge strength.)

5.2 Limit analysis via discontinuity layout optimization

Gilbert *et al.* (2010) presented details of a limit analysis model in which both masonry and soil elements are modelled directly, using the discontinuity layout optimisation (DLO) technique. An advantage of DLO over other comparable techniques (e.g. finite-element limit analysis) is its ability to naturally treat singularities in the stress or displacement fields. The same basic DLO modelling approach as described in Gilbert *et al.* (2010) was applied to the test set-ups considered here, using the LimitState:GEO software (LimitState, 2009). For all simulations: (a) a mobilisation factor of 0.33 was applied to the soil strength except in regions where large soil strains were expected (i.e. in the vicinity of the surface applied loads of test set-ups T4 [APL] and T6 [A-L], where an initial partial bearing capacity failure will ensure soil strains are high); (b) soil

strength along the relatively rough soil–arch interfaces was taken as 0.5 times that of the adjoining soil mass; (c) the relatively smooth interfaces around the extended keystone were modelled with an interface friction angle consistent with that of the test chamber wall (8°). All other material and geometrical parameters were as already indicated.


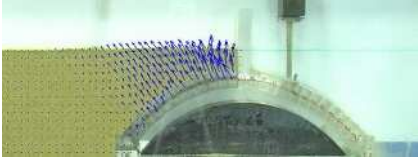
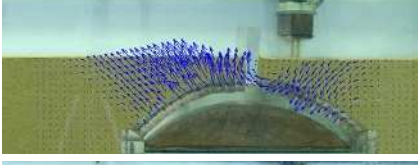



Each analysis took less than a minute to solve on a standard desktop PC when using a comparatively fine numerical discretisation, comprising (nominally) 2000 nodes. For sake of simplicity it was assumed here that (a) all voussoirs were incompressible, and (b) no sliding could occur between voussoirs (this is at variance with the assumptions made in Gilbert *et al.* (2010), where crushing of the masonry and sliding failures were allowed). All numerical results are shown in Table 3. Figure 8 shows two sample DLO predicted failure mechanisms.

It is clear from Table 3 that the numerical predictions are all close to the experimentally recorded peak loads (all within 10% of the experimental results, except in the case of test set-up T4 without the extended keystone which was within 12%). The predicted failure mechanisms also provide insights into the modes of response involved. For example, Figure 8(a) shows the predicted mechanism for test set-up T2 obtained when using DLO, showing the presence of a series of closely spaced inclined slip-lines in the ‘passive zone’, remote from the applied load, which implies that the soil here is subject to an almost uniform state of shear strain. Because of the large volume of soil involved this also implies that soil strains will be comparatively small, effectively explaining why it is necessary to use mobilised rather than peak soil strength here. It is also apparent that by modelling the soil directly using DLO, rather than merely its anticipated effects when using the rigid block limit analysis method, that the extent of the backfill involved in the collapse mechanism becomes clearly evident. The DLO-based limit analysis method also has the advantage that non-standard fill configurations can readily be modelled, with the only real disadvantage being increased computational cost.

In Figure 8(b) the relatively complex patterns of slip-lines in the vicinity of the load are shown. Here the load is effectively free to move until soil strains are large, thus allowing peak soil strength to be mobilised here.

6. Discussion

The fact that load spreading and passive restraint contribute to the live load capacity of a masonry arch bridge is well known, but the precise nature of the various interactions involved have proved difficult to characterise. In this paper the use of novel experimental test set-ups, PIV and both established and

Test [Key*]	Photographs of model bridges with superimposed displacement vectors at peak load	Experimental peak load capacity (N) [results without extended keystone]			Numerical analysis ^a			
					A. Rigid block limit analysis		B. DLO limit analysis	
					Load (N)	Diff ^b	Load (N)	Diff ^b
T1 [---]		107 [104]	108 [104]	107 [106]	99	-7%	105 [96]	-2% [-8%]
T2 [-P-]		141	142	140	134	-5%	145	+3%
T3 [AP-]		138 [137]	137 [135]	137 [138]	132	-4%	136 [132]	-1% [-3%]
T4 [APL]		181 [178]	183 [177]	182 [179]	187	+4%	184 [157]	+1% [-12%]
T5 [A--]		103	104	100	97	-5%	96	-6%
T6 [A-L]		130	131	136	136	+3%	140	+4%

*A = active; P = passive; L = load spreading

^aModel input files available from <http://cmd.shef.ac.uk> and the LimitState:RING and LimitState:GEO analysis software employed is freely available for academic use from <http://www.limitstate.com>.

^bcf. Corresponding mean experimental peak load

Table 3. Experimental peak loads for each test set-up against analysis results (PIV arrow magnification factor = 25)

recently developed limit analysis procedures have helped to shed some light on the situation.

The aim of the numerical analysis comparisons was to assist interpretation of the experimental results. Although for sake of simplicity the relatively simple modelling assumptions used by

previous authors were adopted, reasonably good fit with the experimental results was obtained.

In test set-up T1 the behaviour of the ‘arch only’ model was correctly predicted by both numerical limit analysis methods. Test set-up T2 allowed investigation of the passive resistance

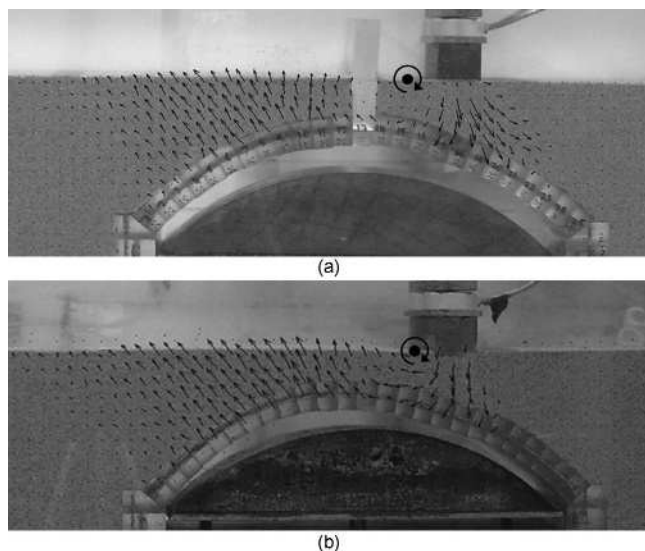


Figure 6. Test set-up T4 displacements, also showing approx. location of instantaneous centre of rotation: (a) with, and (b) without extended keystone (arrow magnification factor = 25)

only situation, indicating an increase in load capacity of approximately 30%. This is consistent with mobilisation of approximately one third of the full theoretical passive pressure, or approximately one third of the soil strength, as indicated by comparing the experimental result with the rigid block and DLO limit analysis results respectively. (For the modelled soil strength, a mobilised soil strength of 0.33 is equivalent to a mobilisation factor of 0.3 on the passive earth pressure coefficient used in the rigid block limit analysis model). It is perhaps worth noting that use of a full mobilised strength would have led to an increase in load capacity of test T1 by approx. 100%, rather than 30%.

Test set-up T3 allowed the effect of fill positioned on the loaded side of the arch to be modelled, though without spreading of the applied load. This indicated a small reduction in load capacity compared with that obtained from test set-up T2, as would be expected since the additional fill exerts an additional disturbing load. While the effect is fairly minor (a decrease of only a few percent in the collapse load), it is predicted to occur in both the rigid block and DLO limit analysis models.

In test set-up T4 the effect of load spreading is also included, by applying the loading at the soil surface. The approximately 30% increase in load capacity was predicted in both the rigid block and DLO limit analysis models. However the DLO analysis model indicated that the load carrying capacity was fairly sensitive to the arch/soil interface factor (Gilbert *et al.*,

2010). (The factor of 0.5 employed here was considered consistent with the relatively rough surface that was present on the extrados surface of the voussoirs.)

Tests set-ups T5 and T6 replicate set-ups T3 and T4 respectively, although with passive resistance effects removed. This resulted in a reduction in load-carrying capacity of approx. 30%, experimentally and in both the DLO and rigid block limit analysis models.

In general very good agreement between the experimental and numerical limit analysis results was obtained, with only one numerical result differing by more than 10% from the corresponding mean experimentally recorded value. However, while the main aim of undertaking the simple numerical studies described herein was to aid interpretation of the experimental observations, should more in-depth 'back analysis' studies be undertaken in future then various refinements to the models could be made. For example, for sake of simplicity the effect of test chamber wall friction was ignored in the numerical analyses described, but could potentially be included. (Hence the fact that the experimentally recorded peak loads are, on average, slightly higher than those indicated in the numerical analyses is to be expected.) Furthermore, considering the DLO simulations specifically, it is possible that the physically unrealistic (dilative) flow rule implicit in plastic limit analysis led to increased predicted capacities being obtained from models involving an extended keystone voussoir and surface loading (i.e. test set-ups T4 and T6). Thus, assuming a numerical analysis model in which this effect can be removed is in future used, it may for example be found that to compensate a higher soil-arch interface roughness needs to be used in the model in order to maintain good agreement with the experiments. Use of a higher soil-arch interface roughness would also increase the predicted load-carrying capacity of the test set-up T4 models not incorporating an extended keystone voussoir, potentially leading to this now lying closer (i.e. less than the current 12%) to the mean experimental result. The aforementioned brief discussion gives a hint of the complexity involved when attempting to manually correlate results from experiments and numerical models, and highlights the need to develop objective automatic correlation schemes; this is the subject of current research.

7. Conclusions

1. The backfill surrounding the barrel of a masonry arch bridge is known to both distribute live load and to provide passive restraint to sway of the arch barrel. This paper has described a novel series of laboratory tests which allow these effects to be isolated. The tests have provided results which should prove valuable for researchers and practitioners wishing to objectively validate numerical analysis models.

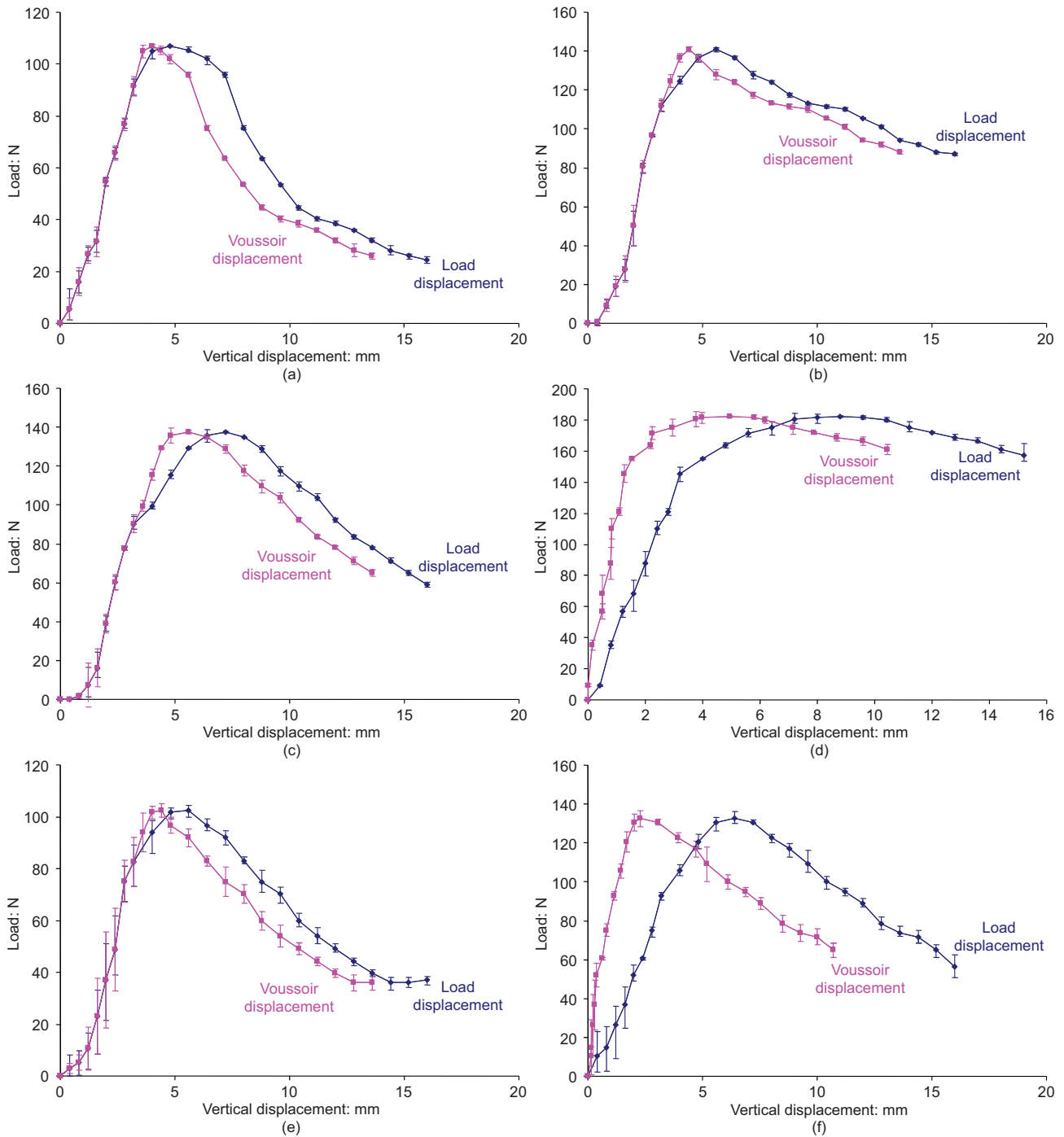


Figure 7. Load–displacement curves for model arch bridge test setups: (a) T1, (b) T2, (c) T3, (d) T4, (e) T5, (f) T6

2. Results indicate that current code of practice recommendations which specify a 2:1 (vertical:horizontal) live load distribution, with uniform pressures then applied to the arch barrel, can lead to non-conservative predictions of

load-carrying capacity. Also, as found in previous research studies, it was found that only approximately one third of the theoretical full theoretical passive pressure was mobilised during the experiments.

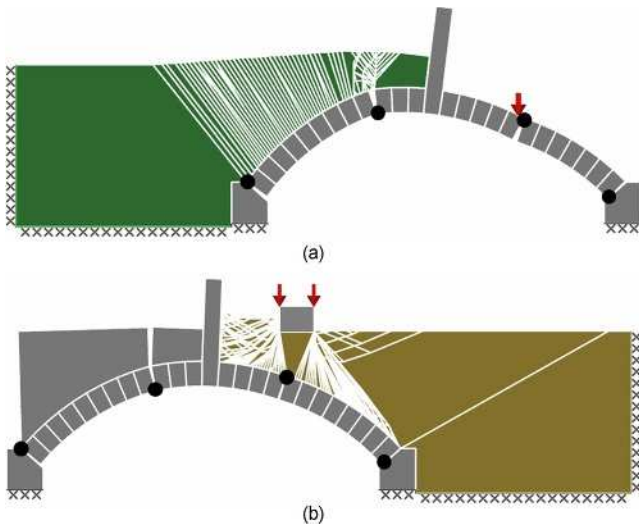


Figure 8. Sample DLO limit analysis output for: (a) set-up T2 (passive restraint only), (b) set-up T6 (load spreading and active pressures)

3. Limit analysis software based on the rigid block method of analysis and incorporating comparatively simple, indirect, models for load spreading and passive restraint effects was found to be capable of producing good predictions of the experimentally observed peak loads (within 10% in all cases).
4. Limit analysis software utilising the DLO procedure was also found to be capable of producing good predictions of the experimentally observed peak loads (within 10% in most cases). However, in the analyses mobilised rather than peak soil strengths needed to be used in regions of low soil strains (e.g. on the side of the bridge remote from the load). This is akin to applying a reduction factor to the coefficient of lateral earth pressure when using simpler limit analysis models. However, the DLO-based limit analysis model has the advantage that non-standard fill configurations can be modelled, and that the extent of the backfill involved in the collapse mechanism is clearly evident.

Acknowledgements

The support of Engineering and Physical Science Research Council (EPSRC) is gratefully acknowledged (firstly for the doctoral studentship held by the first author, and secondly for the Advanced Research Fellowship held by the second author – grant reference GR/S53329). The authors also acknowledge the support provided by Essex County Council.

REFERENCES

Alexander T and Thomson AW (1900) *Scientific Design of Masonry Arches*. Dublin University Press, Dublin, Ireland.

BSI (1986) BS 8004. Section 3: Code of practice for foundations. BSI, Milton Keynes, UK.

Burroughs P, Hughes TG, Hee S and Davies MCR (2002) Passive pressure development in masonry arch bridges. *Proceedings of the Institution of Civil Engineers – Structures and Buildings* **152(4)**: 331–339, <http://dx.doi.org/10.1680/stbu.2002.152.4.331>.

Callaway PA (2007) *Soil–Structure Interaction in Masonry Arch Bridges*. PhD thesis, University of Sheffield, UK.

Chettoe CS and Henderson W (1957) Masonry arch bridges: a study. *Proceedings of the Institution of Civil Engineers* **7(4)**: 723–774, <http://dx.doi.org/10.1680/iicep.1957.2623>.

Davey N (1953) *Tests on Road Bridges*, Department of Scientific and Industrial Research–Building Research Station, London, UK.

Fairfield CA and Ponniah DA (1994) The effect of fill on buried model arches. *Proceedings of the Institution of Civil Engineers – Structures and Buildings* **94(4)**: 358–371, <http://dx.doi.org/10.1680/istbu.1994.27205>.

Gilbert M and Melbourne C (1994) Rigid-block analysis of masonry structures. *The Structural Engineer*. **72(21)**: 356–361.

Gilbert M, Smith CC, Wang J, Callaway P and Melbourne C (2007) Small and large-scale experimental studies of soil–arch interaction in masonry bridges. *Proceedings of the 5th International Arch Bridges Conference, Madeira*, pp. 381–388.

Gilbert M, Smith CC and Pritchard TJ (2010) Masonry arch analysis using discontinuity layout optimisation. *Proceedings of the Institution of Civil Engineers – Engineering and Computational Mechanics*. **163(3)**: 155–166, <http://dx.doi.org/10.1680/eacm.2010.163.3.155>.

Harvey WJ (2006) Some problems with arch bridge assessment and potential solutions. *The Structural Engineer* **84(3)**: 45–50.

Head KH (1982) *Manual of Soil Laboratory Testing*. Pentech Press, Plymouth, UK.

Highways Agency (2001a) *Design Manual for Roads & Bridges: BA 16/97 The Assessment of Highway Bridges and Structures*. HA, London, UK.

Highways Agency (2001b) *Design Manual for Roads and Bridges: BD21/01 The Assessment of Highway Bridges and Structures*. HA, London, UK.

Hulet KM, Smith CC and Gilbert M (2006) Load-carrying capacity of flooded masonry arch bridges. *Proceedings of the Institution of Civil Engineers – Bridge Engineering* **159(3)**: 97–103, <http://dx.doi.org/10.1680/bren.2006.159.3.97>.

LimitState (2009) *LimitState:GEO Manual*, Version 2.0. LimitState, Sheffield, UK.

LimitState (2011) *LimitState:RING Manual*, Version 3.0. LimitState, Sheffield, UK.

Livesley RK (1978) Limit analysis of structures formed from rigid blocks. *International Journal for Numerical Methods in Engineering* **12(12)**: 1853–1871.

-
- Melbourne C and Gilbert M (1995) The behaviour of multi-ring brickwork arch bridges. *The Structural Engineer* **73(3)**: 39–47.
- Network Rail (2006) *The Structural Assessment of Underbridges*. Network Rail, London, UK, Guidance Note NR/GN/CIV/025
- Smith CC, Gilbert M and Callaway PA (2004) Geotechnical issues in the analysis of masonry arch bridges. *Proceedings of the 4th International Arch Bridges Conference, Barcelona, Spain*, pp. 343–352.
- Wang J and Melbourne C (2010) Mechanics behind the MEXE method for masonry arch assessment. *Proceedings of the Institution of Civil Engineers – Engineering and Computational Mechanics* **163(3)**: 187–202, <http://dx.doi.org/10.1680/eacm.2010.163.3.187>.
- White DJ, Take WA and Bolton MD (2001) Measuring soil deformation in geotechnical models using digital images and PIV analysis. *Proceedings of the 10th International Conference on Computer Methods and Advances in Geomechanics, Tuscon, USA*, pp. 997–1002.

WHAT DO YOU THINK?

To discuss this paper, please email up to 500 words to the editor at journals@ice.org.uk. Your contribution will be forwarded to the author(s) for a reply and, if considered appropriate by the editorial panel, will be published as discussion in a future issue of the journal.

Proceedings journals rely entirely on contributions sent in by civil engineering professionals, academics and students. Papers should be 2000–5000 words long (briefing papers should be 1000–2000 words long), with adequate illustrations and references. You can submit your paper online via www.icevirtuallibrary.com/content/journals, where you will also find detailed author guidelines.